Optical buffers based on slow light in electromagnetically induced transparent media and coupled resonator structures: comparative analysis

Jacob B. Khurgin

Department of Electrical and Computer Engineering, Johns Hopkins University, Baltimore, Maryland 21218

Received July 21, 2004; revised manuscript received October 22, 2004; accepted December 3, 2004

The optical buffer is a key component in all-optical information processing systems. Recently a number of schemes that use slow light propagation in various media and structures have been proposed as means toward implementation of all-optical buffers. We rigorously analyze the similarities and differences in approaches that use electromagnetically induced transparency (EIT) and coupled resonant structures (CRS). We introduce the figure of merit, finesse, that is common to both approaches and obtain fundamental limitations on bit rates and storage capacities of optical buffers. We show that at very low bit rates and storage capacities EIT outperforms CRS, but at rates of 10 Mbits/s and above the EIT medium becomes quite inefficient, and the situation is reversed. Two types of CRS based on high-index-contrast fiber gratings and high-index semiconductor–air photonic crystals and (or) microring resonators are found to hold promise for applications in the 1–1000-Gbits/s range, but only if the losses can be drastically reduced.

OCIS codes: 210.0210, 200.4740, 260.0260.

1. INTRODUCTION

Recent years have seen rapid development in the area of optical communications. Advances in optical amplifiers and passive optical components such as add–drop filters have eliminated large numbers of electronic regeneration steps that limited the system speed and capacity. Unfortunately the most sophisticated steps of switching and routing are still handled electronically, although substantial effort has been expended in the quest for an all-optical implementation of these functions. Any all-optical processor must include an optical buffer as one of its most important enabling components. The purpose of the optical buffer is to store and then release the data in optical format without conversion into the electrical format. Despite the ostensible simplicity of this task, the optical buffer has always been and still remains a major stumbling block on the way to all-optical processing. This is easy to understand since the term "buffering" implies, at the physical level, localization, and photons, being particles with zero rest mass, are far less amenable to localization than electrons. For this reason the only practical optical buffers remain the fiber loop[1] or its close cousin, the folded, free-space delay line in which the delay time is accumulated by propagation over a long optical path.

In future networks with optical packet routing the optical data would need to be stored for times that are equal to at least the packet length. Assuming that the packet length is of the order of 1000 bits and the data rate is of the order of 10 Gbits/s, the length of the delay line must be of the order of 20–30 m, depending on the refractive index. Resorting to such bulky components would negate all the advantages in size and weight expected from doing all-optical processing. There exists another important field of microwave photonics—microwave phased-array antennae—where optical, true-time delay lines hold promise of reducing the size and weight of components. Although the length of the true-time delay line does not need to exceed the wavelength of the RF signal, i.e., a few centimeters at best, there are still significant benefits in a scheme that would allow one to reduce that length further.

Reducing the length of the optical buffer while keeping the total delay time constant implies reduction of group velocity. Group velocity can be reduced by using strong resonances in either time or space that cause coupling of energy between either counterpropagating electromagnetic waves or between electromagnetic and other forms of energy. Indeed the last decade has seen an increased interest in slowing photons by using two alternative approaches to "storing" the photons. The older one is the optical delay line,[2] in which the light path is lengthened by forcing the light to retrace its path through repeated reflections in grating,[3] coupled-ring resonators,[4] or coupled defect modes in photonic crystals.[5–10] In all these structures the group velocity of light is slowed in the vicinity of a sharp resonance in the reflection that limits the effective bandwidth of the delay line because of quadratic dispersion. Quadratic dispersion, however, can be canceled when cascaded[11] or Moire gratings[12] are used; yet, as will be shown in this paper the residual third-order dispersion still limits the bandwidth. It can be argued that most if not all of these slow-light schemes can be treated as propagation in coupled resonators.[13] In order to incorporate as wide a range of different structures as possible, we will refer to these designs as coupled resonator structures (CRS).

0740-3224/05/051062-13/$15.00

The more recent approach to slowing light based on use of dispersion in the vicinity of sharp atomic resonances has generated much excitement. Usually, absorption is quite high near the resonance, but if a strong optical field splits the resonance in two, the absorption becomes anomalously low. This is electromagnetically induced transparency, or EIT. EIT was first observed in 1991,[14] and its ability to reduce the velocity of light was explored by Harris *et al.*[15] and Kasapi *et al.*[16] shortly afterward.[15,16] EIT slowed the light to less than 10 m/s in metal vapors[17,18] and less than 45 m/s in the solid state.[19] More recently light was effectively stopped in the EIT medium,[20,21] and the proposal was made[22] for slowing light through EIT in semiconductor quantum dots (QDs).

Both CRS and EIT schemes have strong advocates who prefer to point out their differences rather than their considerable similarities. To the best of our knowledge there is no comprehensive comparison of the two approaches that can answer the practical question: What benefits do CRS and EIT slow-light schemes offer for storage of optical packets of given symbol rate B and length N_{st} symbols per packet? In other words, how much can the group velocity of light be slowed before dispersion causes excessive intersymbol interference that leads to data loss?

In this paper we provide clear answers to this and other important questions by the use of simple analytical expressions. We point out that while EIT and CRS are remarkably similar to one another, they have different group-index-versus-bandwidth dependences that cause CRS to perform better at high bit rates. We are concerned here only with the fundamental limitations to the performance of slow-light buffers imposed, as we shall see, by third-order dispersion β_3. Of course, in the near future, losses due to imperfections in fabrication (for CRS) or inhomogeneous broadening (for EIT) will continue to be the dominant limiting factors, but here our goal is to determine the theoretical upper bound of the performance of the slow-light schemes. We show that even if all the fabrication issues are resolved this performance will be inherently limited by dispersion.

2. EIT: SLOW LIGHT BASED ON RESONANT OPTICAL TRANSITIONS

A. Dispersion near Single Resonance: Polariton

The fact that electromagnetic radiation experiences a large change in its group velocity in the vicinity of a strong resonance is well known. In optics this phenomenon is usually referred to as strong dispersion, while in solid-state physics it is more often described as a polariton effect. Resonance, shown in Fig. 1(a), can be associated with excitation of a strong atomic transition in a gas medium, of an exciton in a semiconductor (exciton polariton), of a plasmon in metal (plasmon polariton), or of a polar lattice vibration (phonon polariton). One can characterize this excitation of matter as a polarization wave with its frequency ω_{12} independent (or nearly independent in comparison with a photon) of its wave vector k as shown in Fig. 1(b) next to the dispersion of a photon. We have

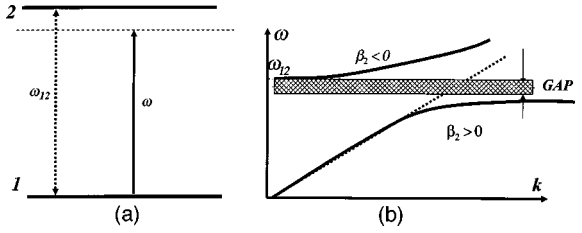

Fig. 1. (a) Two-level resonant atomic system, (b) the dispersion of the slow wave (polariton).

$$k = \frac{\omega \bar{n}}{c}, \tag{1}$$

where $\bar{n}$ is the background refractive index of the medium considered to be constant within a narrow frequency range. The two waves—electromagnetic (photon) and polarization—interact with an interaction strength that is proportional to the dipole matrix element of the transition μ_{12}. The interaction becomes very strong in the vicinity of resonant frequency ω_0 when the energy couples back and forth between two waves. The coupled-waves description is the semiclassical picture of anomalous dispersion; in the full quantum theory one can describe it as a formation of a mixed quasi-particle (or polariton) that combines properties of both photon and matter excitation.[23] The polariton dispersion is shown in Fig. 1(b); it consists of two branches with the gap between them corresponding to the region of negative dielectric susceptibility where the electromagnetic waves cannot propagate. Near the resonance the group velocity of the polariton,

$$v_g = \frac{\partial \omega}{\partial k}, \tag{2}$$

is greatly reduced, since most of the energy of the polariton at these frequencies is contained in the stationary matter excitation rather than in the moving electromagnetic wave.

The obvious idea for using strong matter resonance to slow the light has two major drawbacks that reduce its practicality. First the transitions have strong absorption within finite linewidth:

$$\gamma_{12} \approx 1/T_2^{(12)}, \tag{3}$$

where $T_2^{(12)}$ is a coherence time. Second the group velocity changes rapidly in the vicinity of resonance. This change is usually gauged by group-velocity dispersion (GVD), also referred to as second-order dispersion,

$$\beta_2 = \frac{\partial v_g^{-1}}{\partial \omega} = \frac{\partial^2 k}{\partial \omega^2}, \tag{4}$$

and it can cause rapid loss of information in the signal.

As one can see in Fig. 1(a) the GVD has opposite sign below and above the resonance. Therefore if one could operate in the region between two equally strong transitions their second-order dispersions would cancel each other leaving only the third-order dispersion,

$$\beta_3 = \frac{\partial^3 k}{\partial \omega^3} > 0, \tag{5}$$

which is positive irrespective of whether one operates below or above resonance. However, β_3 has a weaker impact on signal quality than β_2. This dispersion-compensated scheme is straightforward and appealing, but unfortunately, suitable media with two closely spaced strong and narrow resonances are difficult to find in nature. EIT, on the other hand,[14] provides an ingenious way to avoid the constraints imposed by nature and to create artificially the proper medium using the "dressed states."

B. Dispersion near Twin Resonances: EIT

Consider a typical EIT scheme, usually referred to as a Λ scheme[24] and shown in Fig. 2(a). The upper level A is split into two "dressed" levels A_1 and A_2 by the pump light originating from level B. The splitting is equal to 2Ω, where $\Omega = \mu_{AB}E_P/\hbar$ is the Rabi frequency, μ_{AB} is the matrix element of the electrical dipole, and E_P is the pumping optical field. The probe light is at frequency ω close to the resonance between the ground level G and original level A. The dielectric constant in the vicinity of the resonance is

$$\epsilon(\delta\omega) = \bar{n}^2 + \frac{N\mu_{AG}{}^2}{\hbar\epsilon_0}\frac{\delta\omega + i\gamma_{BG}}{\Omega^2 - (\delta\omega + i\gamma_{BG})(\delta\omega + i\gamma_{AG})}, \tag{6}$$

where $\delta\omega = \omega - \omega_0$ is detuning, N is the concentration of active ions or atoms, and γ_{AG} and γ_{BG} are the broadenings. Note that γ_{GB} is the broadening of the transition $G \rightarrow B$ that can be forbidden and thus is quite narrow. Herein lies the second advantage of the EIT medium: the absorption can be reduced substantially by quickly transferring the photon energy into the matter excitation that is well isolated from the outside world and thus has long coherence time. This fact distinguishes EIT from other seemingly analogous methods of slowing light by use of coherent population pulsations.[25] From Eq. (6) the complex refractive index can be found as

$$\tilde{n}(\delta\omega) = [\epsilon(\delta\omega)]^{1/2} = \bar{n} + \frac{Ne^2 f_{AG}}{4\bar{n}m_0\omega_0\epsilon_0}\frac{\delta\omega + i\gamma_{BG}}{\Omega^2 - (\delta\omega + i\gamma_{BG})(\delta\omega + i\gamma_{AG})}, \tag{7}$$

where f_{AG} is the oscillator strength. We can also define a modified (by a factor $2\bar{n}$) plasma frequency as

$$\Omega_p{}^2 = \frac{Ne^2 f_{AG}}{4\bar{n}^2 m_0\epsilon_0}. \tag{8}$$

With Eq. (7) one can plot the dispersion curve for the EIT medium [Fig. 2(b)]—as one can see the curve is "squeezed and flattened" between two forbidden gaps associated with resonances. The curve is plotted in the limit of zero broadenings—their inclusion would only change the curve near the Rabi-split resonances and not in the region of interest near ω_0. Clearly, as the transparency region becomes narrower the group velocity becomes progressively smaller. We can obtain the expression for the group index at the center of the transparency region ($\delta\omega = 0$) as

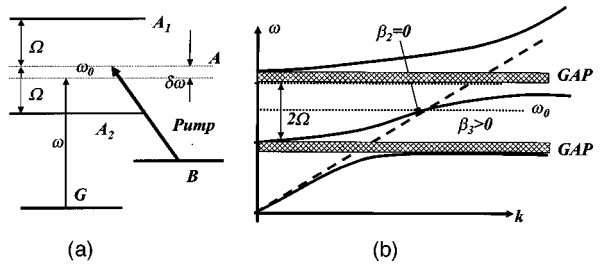

Fig. 2. EIT in the Λ scheme: (a) atomic-level diagram, (b) dispersion of the slow wave.

$$n_g(0) = c\frac{\partial k}{\partial \omega} = \bar{n} + \omega\,\mathrm{Re}\left.\frac{\partial \tilde{n}}{\partial \omega}\right|_{\delta\omega=0} = \bar{n} + \bar{n}\Omega_p{}^2\frac{\Omega^2 - \gamma_{BG}{}^2}{(\Omega^2 + \gamma_{BG}\gamma_{AG})^2}, \tag{9}$$

and also find the absorption coefficient as

$$\alpha(0) = 2\frac{\omega}{c}\,\mathrm{Im}\,(\tilde{n})|_{\delta\omega=0} = 2\bar{n}\frac{\Omega_p{}^2}{c}\frac{\gamma_{BG}}{\Omega^2 + \gamma_{BG}\gamma_{AG}}. \tag{10}$$

Now we can determine the upper limit placed by the absorption on the delay time as

$$t_{abs} = n_g \ln 2/(\alpha c) \approx \frac{\ln 2}{2}\gamma_{GB}{}^{-1}\frac{\Omega^2 - \gamma_{BG}{}^2}{\Omega^2 + \gamma_{BG}\gamma_{AG}}, \tag{11}$$

i.e., the time over which half of the optical power gets dissipated. We shall refer to t_{abs} as "absorption time." In Eq. (11) we have neglected the "background" time delay not associated with EIT resonances because we are interested only in the regime of large group index. Maximum time delay can be achieved for large Rabi splitting and is equal simply to

$$t_{abs,max} = \frac{\ln 2}{2}\gamma_{BG}{}^{-1}, \tag{12}$$

and thus roughly equals the coherence time of the "isolated" excitation $G \rightarrow B$. This result is quite logical considering that optical energy is transferred into the coherent excitation of that transition. Of course as the Rabi frequency approaches infinity, the group index decreases to its background value. A more interesting observation thus would be to see what value of group index can be achieved for a given absorption time. Solving Eqs. (9) and (11) together we obtain

$$\frac{n_g}{\bar{n}}(t_{abs}) = 1 + \frac{2}{\ln 2}\Omega_p{}^2 t_d(\gamma_{BG} + \gamma_{AG})^{-1}\left(1 - \frac{t_{abs}}{t_{abs,max}}\right) = 1 + \Omega_p{}^2 t_{abs}t_{AG}\left(1 - \frac{t_{abs}}{t_{abs,max}}\right), \tag{13}$$

where $t_{AG} = 2/\ln 2(\gamma_{AG} + \gamma_{BG})^{-1} \approx 2/\ln 2\,\gamma_{AG}{}^{-1} \sim T_{2,A}$. As one can see the group index reaches its maximum when

$$t_{abs} = 1/2t_{abs,max}, \tag{14}$$

or

$$\Omega_{max} = [\gamma_{BG}(\gamma_{AG} + 2\gamma_{BG})]^{1/2} \approx (\gamma_{BG}\gamma_{AG})^{1/2}$$

and

$$\frac{n_{g,\max}}{\bar{n}} = 1 + 1/4\Omega_p{}^2 t_{\mathrm{abs,max}} t_{AG}. \quad (15)$$

Thus the total number of bits that can be stored in the EIT medium $N_{st}=t_{abs}B$ increases with the bandwidth B if nothing but the residual absorption in the EIT band is taken into account. The situation changes drastically once we introduce bandwidth limitations.

First we neglect the residual absorption in Eq. (9) and obtain

$$n_g{}^{(\mathrm{EIT})}(0) = \bar{n} + \bar{n}\frac{\Omega_p{}^2}{\Omega^2}. \quad (16)$$

If one wants to avoid the absorption of high-frequency components of the signal, the width of the EIT region 2Ω must be at least larger than the bandwidth of the signal $\Delta\omega$, proportional to the symbol rate. Thus we can rewrite Eq. (16) as

$$n_g{}^{(\mathrm{EIT})}(0) = \bar{n} + \bar{n}\frac{\Omega_p{}^2}{a^2B^2}, \quad (17)$$

where a is a constant of the order of unity, depending on the exact shape of the signal.

At this point we can actually estimate the values of plasma frequency for different media and compare them, as shown in Table 1. In the original paper by Harris *et al.*[15] ^{208}Pb vapor was used with concentration $N\approx 7\times10^{15}$ cm^{-3} and oscillator strength $f_{AG}\approx 0.2$, resulting in $\Omega_p\approx 10^{12}$ s^{-1}. EIT was observed in this medium in 1995[16] but at a much smaller density $N\approx 2\times10^{15}$ cm^{-3}. In the other gas-phase media where EIT had been observed, in Sr^{+}[14] and in ^{87}Rb,[20,21,24,26] the combinations of atomic density and oscillator strength are not as favorable as in lead vapor. For a solid-state medium such as $Pr^{3+}:Y_2SiO_5$ (PrYSO) in which EIT has been demonstrated,[19] the concentration of active atoms is much higher, $N\approx 7\times10^{19}$ cm^{-3}, but the oscillator strength of the transition is much lower,[27] $f_{AG}\approx 3\times10^{-7}$, resulting in $\Omega_p\approx 4\times10^{10}$ s^{-1}. Finally for the QD medium suggested in Ref. 22 the concentration can be as high as 10^{16} cm^{-3}, while the oscillator strength can actually be larger than unity as a result of lower effective mass. Assuming $f_{AG}\approx 10$ we can obtain very high values of plasma frequency, up to $\Omega_p\approx 5\times10^{12}$ s^{-1}. But the maximum delay time in the QD medium is limited to less than a nanosecond even at low temperature because of scattering.

Judging from Eq. (17) sufficiently high group index enhancement (of the order of 100 or more) can be achieved for symbol rates of the order of $\Omega_p/10a$, i.e., up to a few hundred gigabits/s for QD media and a few gigabits/s for the rare-earth-doped medium. But these results are to change drastically once dispersion is introduced.

Table 1. Performance Characteristics of Various EIT Slow-Light Optical Buffers

Medium	^{208}Pb	Sr^{+}	^{87}Rb	PrYSO	QDs
N (cm^{-3})	7×10^{15}	2×10^{14}	2×10^{12}	7×10^{19}	10^{16}
f_{AG}	0.2	0.15	0.1	3×10^{-7}	10
Ω_p (s^{-1})	10^{12}	1.4×10^{11}	1.2×10^{10}	4×10^{10}	5×10^{12}
$T_{\mathrm{abs,max}}$ (s)	0.4×10^{-7}	1.3×10^{-9}	1.6×10^{-7}	0.3×10^{-3}	0.4×10^{-9}
F_{EIT}	4×10^{4}	200	2×10^{3}	1.2×10^{7}	2×10^{3}
$N_{\mathrm{st,max}}$	200	6	28	8×10^{3}	28
$B_{\mathrm{max,cap}}$,	5 G[a]	4 G	169 M	25 M	5 G
Performance with storage capacity of 10 bits					
$B_{\mathrm{max}}^{(\mathrm{EIT})}$	23 G	3 G	280 M	0.9 G	110 G
$n'_{g,\mathrm{max}}$	9×10^{3}	—	21	2×10^{9}	22
$B_{\mathrm{min}}^{(\mathrm{EIT})}$	250 M	7 G	63 M	33 k	25 G
L_{EIT} (cm)	0.13	—	229	0.002	0.15
Performance with storage capacity of 50 bits					
$B_{\mathrm{max}}^{(\mathrm{EIT})}$	10 G	—	—	0.4 G	—
$n'_{g,\mathrm{max}}$	72	—	—	2×10^{6}	—
$B_{\mathrm{min}}^{(\mathrm{EIT})}$	1.25 G	—	—	0.3 M	—
L_{EIT} (cm)	16	—	—	0.25	—
Performance with storage capacity of 200 bits					
$B_{\mathrm{max}}^{(\mathrm{EIT})}$	6 G	—	—	300 G	—
$B_{\mathrm{min}}^{(\mathrm{EIT})}$	5 G	—	—	0.6 M	—
$n'_{g,\mathrm{max}}$	2.5	—	—	10^{4}	—
L_{EIT} (cm)	285	—	—	88	—

[a]Units K, M, G stand for kilo-, mega-, gigabits/second.

C. Third-Order Dispersion

First find the second-order dispersion:

$$\beta_2^{(\mathrm{EIT})}(\delta\omega) = c^{-1}\frac{\mathrm{d}}{\mathrm{d}(\delta\omega)}[(\omega_0+\delta\omega)n(\delta\omega)] = \frac{2{\Omega_\mathrm{p}}^2\bar{n}c^{-1}}{\Omega^2-\delta\omega^2}\left[\frac{1}{\omega_0}+\delta\omega\frac{3\Omega^2+\delta\omega^2}{(\Omega^2-\delta\omega^2)^2}\right]. \quad (18)$$

As expected the second-order dispersion goes to zero at roughly $\delta\omega \approx \Omega^2/\omega_0$, i.e., close to the middle of the EIT band. The third-order dispersion is always positive and is equal to

$$\beta_3^{(\mathrm{EIT})}(0) = c^{-1}\left.\frac{d\beta_2^{(\mathrm{EIT})}(\delta\omega)}{d(\delta\omega)}\right|_{\delta\omega=0} = \frac{6{\Omega_\mathrm{p}}^2\bar{n}c^{-1}}{\Omega^4}. \quad (19)$$

Now it is the pair of Eqs. (16) and (19) that determines the properties of the EIT slow-light medium. Using them, we can find out the limitations imposed by the third-order dispersion. According to Ref. 28, for a typical return-to-zero on-off-keying Gaussian signal the maximum distance that it can propagate in the presence of third-order dispersion is determined from the relation

$$B[\beta_3 L_{\max}]^{1/3} < \gamma = 0.324. \quad (20)$$

The exact value of γ in inequality (20) may change as a function of modulation format and detection method, but not by much. Also, for on–off-keying the symbol rate and bit rate are identical, so from here on we shall refer to B as the bit rate, understanding that rigorously it should be referred to as symbol rate. The maximum delay can be estimated as

$$t_{\mathrm{d,max}} = \frac{L_{\max}}{c}n_g = \frac{\gamma^3}{B^3 c\beta_3}n_g = \frac{\gamma^3\Omega^2}{6B^3}\left(1+\frac{\Omega^2}{{\Omega_\mathrm{p}}^2}\right), \quad (21)$$

and the maximum number of bits that can be stored then is simply

$$N_\mathrm{st} = Bt_{\mathrm{d,max}} = \frac{\gamma^3\Omega^2}{6B^2}\left(1+\frac{\Omega^2}{{\Omega_\mathrm{p}}^2}\right) = \frac{\gamma^3\Omega^2}{6B^2}\frac{n_g}{n_g-\bar{n}}. \quad (22)$$

We now obtain a far more restrictive relation between the bandwidth and the half-width of the EIT region required to accommodate it.

$$\Omega = 6^{1/2}\gamma^{-3/2}{N_\mathrm{st}}^{1/2}\frac{n_g-\bar{n}}{n_g}B \approx 13.2{N_\mathrm{st}}^{1/2}\frac{n_g-\bar{n}}{n_g}B. \quad (23)$$

For a large slowing factor the index-dependent term in Eq. (23) approaches unity, and one can see how wide the EIT region should be to store a large number of bits. For instance to store just 100 bits of information the ratio between Ω and B becomes 130 rather than a factor of a few that followed from the simpler considerations that led to (17). Substituting Eq. (23) into Eq. (16) we obtain

$$\frac{n_g^{(\mathrm{EIT})}}{\bar{n}} = 1+\frac{{B_{\mathrm{EIT,max}}}^2}{B^2}\frac{n_g^{(\mathrm{EIT})}}{n_g^{(\mathrm{EIT})}-\bar{n}}, \quad (24)$$

where the maximum bit rate of the EIT buffer,

$$B_{\mathrm{EIT,max}}(N_\mathrm{st}) = \frac{\gamma^{3/2}}{6^{1/2}}\Omega_\mathrm{p}N_\mathrm{st}^{-1/2} = 0.075\Omega_\mathrm{p}N_\mathrm{st}^{-1/2}, \quad (25)$$

is defined here as the bandwidth at which the packet containing N_st bits can be slowed down by a factor of ≈ 2.6 according to the general solution of Eq. (25)

$$\frac{n_g^{(\mathrm{EIT})}}{\bar{n}}N_\mathrm{st} = \frac{1}{2}\frac{{B_{\mathrm{EIT,max}}}^2}{B^2}+1+\frac{1}{2}\frac{{B_{\mathrm{EIT,max}}}^2}{B^2}\left(1+\frac{4B^4}{{B_{\mathrm{EIT,max}}}^4}\right)^{1/2} \approx \begin{cases}\dfrac{{B_{\mathrm{EIT,max}}}^2}{B^2}+2 & B \ll B_{\mathrm{EIT,max}} \\ \dfrac{B_{\mathrm{EIT,max}}}{B}+1 & B \gg B_{\mathrm{EIT,max}}\end{cases}. \quad (26)$$

Thus the total length of the EIT buffer required to store N_st bits at a given bit rate B for the case of $B \ll B_{\mathrm{EIT,max}}$ becomes

$$L_{\mathrm{EIT}}(N_\mathrm{st},B) = \frac{cN_\mathrm{st}B^{-1}}{n_g^{(\mathrm{EIT})}} \approx \frac{6c}{\gamma^3\bar{n}}\frac{{N_\mathrm{st}}^2B}{{\Omega_\mathrm{p}}^2}, \quad (27)$$

whereas for high bit rates $B \gg B_{\mathrm{EIT,max}}$ it asymptotically approaches

$$L_0(N_\mathrm{st},B) = \frac{cN_\mathrm{st}B^{-1}}{\bar{n}}. \quad (28)$$

We can also now define the bit rate at which the packet containing N_st bits can be slowed down by a factor $n_g' = n_g/\bar{n}$

$$B_{\mathrm{EIT}}(N_\mathrm{st}n_g') \approx \frac{\gamma^{3/2}}{6^{1/2}}(N_\mathrm{st}n_g')^{-1/2}\Omega_\mathrm{p} \approx 0.075(N_\mathrm{st}n_g')^{-1/2}\Omega_\mathrm{p}. \quad (29)$$

D. Limitations Due to Dephasing: Definition of Finesse

At the same time, from the considerations of the residual loss of Eq. (12) the minimum bit rate at which this can be accomplished becomes

$$B_{\mathrm{EIT,min}}(N_\mathrm{st}) = N_\mathrm{st}/t_{\mathrm{abs,max}}. \quad (30)$$

Of course $t_{\mathrm{abs,max}} \sim \gamma_{GB}^{-1}$ is the upper limit on the absorption time under assumption that $\Omega^2 \gg \gamma_{AG}\gamma_{BG}$ (11). Using Eqs. (23) we can show that this condition is satisfied for as long as

$$\gamma_{AG} \ll 200{N_\mathrm{st}}^3\gamma_{BG}. \quad (31)$$

If the broadening of transition AG is larger than that, the impact of absorption on the performance of the EIT delay line will be even stronger than discussed here.

Combining Eq. (29) and Eq. (31) and we obtain the value of the maximum group-velocity reduction factor attainable:

$$n_{g,\max}'(N_{\rm st}) = \frac{\gamma^3}{6}\frac{F_{\rm EIT}^{\ 2}}{N_{\rm st}^{\ 3}}, \tag{32}$$

where we have introduced the finesse of the EIT transition as

$$F_{\rm EIT} = \Omega_{\rm p} t_{\rm d,max}. \tag{33}$$

We can now see that EIT buffers can effectively slow a packet of $N_{\rm st}$ bits within the range of bit rates $\{B_{\rm EIT,min}(N_{\rm st}), B_{\rm EIT,max}(N_{\rm st})\}$. The lower boundary of the range is determined by the residual absorption, while the upper boundary is determined by the dispersion. As packet length increases the effective range narrows until the maximum packet length,

$$N_{\rm st,max} = \frac{\gamma}{6^{1/3}} F_{\rm EIT} = 0.18 F_{\rm EIT}^{\ 2/3}, \tag{34}$$

is attained. The packet of length $N_{\rm st,max}$ is slowed by a factor of 2.6, and this reduction is achieved at the bit rate of maximum capacity

$$B_{\rm max,cap} = N_{\rm st,max}/t_{\rm d,max} = \frac{\gamma}{6^{1/3}}\Omega_{\rm p}^{\ 2/3} t_{\rm d,max}^{-1/3} \tag{35}$$

It is instructive to reflect on the physical meaning of finesse. If one considers an electromagnetic wave resonantly coupled to an ensemble of atomic dipoles oscillating at frequency ω_0 the energy will be transferred back and forth between the wave and dipoles with the angular frequency $\Omega_{\rm p}$. Therefore, finesse $F_{\rm EIT} \sim \Omega_{\rm p} T_2^{BG}$ is simply the number of times the energy can be moved between the wave and dipoles before the collective polarization of the dipoles decays.

E. Parameters for the Specific EIT Schemes

Let us look at the finesse and capacities of the specific media shown in Table 1. Of all the media PrYSO has the highest finesse and thus the largest storage capacity. In fact, it follows from (32) that $n_{g,\max}'(N_{\rm st}) \sim 10^{12} N_{\rm st}^{-3}$, and one can store a thousand-bit-long packet with group velocity reduced a thousand-fold. Unfortunately, this reduction will take place at a rate of a few kilobits/s and require an unrealistically long medium. But 50 bits can be stored successfully at a bit rate of a few hundred kilobits/s.

Among the gas-phase EIT media, ^{208}Pb originally suggested by Harris *et al.* for group-velocity reduction[15] holds the most promise—it may store about a dozen bits in a realistic length, but regrettably EIT in this medium has been observed experimentally only at lower concentrations,[15] leading to less impressive results than predicted. The more common Sr and Rb vapors offer performance that is far inferior to Pb vapor.

For the QD medium, we obtain, assuming a rather unrealistic value of $t_{\rm d} \sim 400$ ps (1-meV linewidth), a finesse of nearly 2000; thus $n_{g,\max}'(N_{\rm st}) \sim 2 \times 10^4 N_{\rm st}^{-3}$. It follows that a small, 10-bit packet can be slowed down by a respectable factor of 20 at a 20-gigabit/s rate, but for practical packets containing more than 30 bits there is no way of achieving group-velocity reduction at any bit rate in a QD medium. If one takes a more reasonable value of broadening, say 50 meV, finesse becomes only 40, and at most one would be able to store two bits of information in such a buffer. If the broadening exceeds 150 meV—something that one should realistically expect to happen at room temperature—the QD buffer becomes completely ineffective, as it can not store even one bit of information by reducing group velocity.

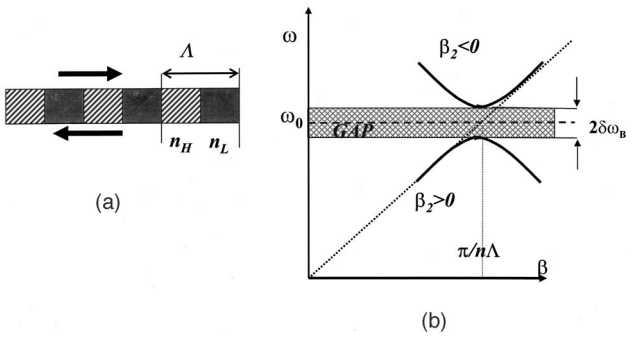

Fig. 3. (a) Bragg reflector, (b) its dispersion.

3. COUPLED RESONATOR STRUCTURES: SLOW LIGHT BASED ON RESONANCES IN SPACE

A. Fiber Bragg Grating as a Slow-Wave Medium

Let us now turn our attention to a different method of reducing the group velocity of light. Consider for instance the Bragg reflector composed of alternating layers of high ($n_{\rm H}$) and low ($n_{\rm L}$) effective refractive index with period Λ shown in Fig. 3(a). The Bragg reflector can be implemented in waveguide, fiber, or in traditional thin-film technology. The dispersion of the Bragg reflector, shown in Fig. 3(b), exhibits a photonic bandgap near the Bragg frequency $\omega_0 = c/\bar{n}\Lambda$ having half-width

$$\delta\omega_{\rm B} = \omega_0 \frac{2}{\pi} \sin^{-1}\left(\frac{n_{\rm H} - n_{\rm L}}{n_{\rm H} + n_{\rm L}}\right). \tag{36}$$

The group velocity in the vicinity of the photonic bandgap is reduced as

$$n_g \sim \frac{\bar{n}|\omega - \omega_0|}{\sqrt{(\omega - \omega_0)^2 - \delta\omega_{\rm B}^{\ 2}}}. \tag{37}$$

The reduction in group velocity is accompanied by a very large increase in the second-order dispersion,

$$\beta_2 = {\rm sign}(\omega_0 - \omega)\frac{\bar{n}}{c}\frac{\delta\omega_{\rm B}^{\ 2}}{[(\omega - \omega_0)^2 - \delta\omega_{\rm B}^{\ 2}]^{3/2}}, \tag{38}$$

which renders the simple Bragg reflector an inefficient delay line.

B. Coupled Resonator Structures

One should note, however, that the sign of β_2 is different below and above Bragg resonance, just as in the case of atomic resonance [Eq. (4)]. Thus if one combines two reflectors with different Bragg frequencies ω_{01} and ω_{02} one can cancel β_2 in the vicinity of $\omega_0 = (\omega_{01} + \omega_{02})/2$. The cancellation can be achieved by cascading two gratings[11] or by using two gratings superimposed onto each other in a Moiré pattern.[12] The latter is of course equivalent to pe-

riodic modulation of the reflectivity, i.e., essentially equivalent to a periodic array of coupled Fabry–Perot cavities, as shown Fig. 4(a). Clearly one can use different types of resonators to achieve the same effect of reducing group velocity and simultaneously cancelling β_2, such as, for instance, the coupled microdisk or microring resonators[13] shown in Fig. 4(b) or the coupled defect modes in photonic crystals[6–10] shown in Fig. 4(c).

Although implementation methods are different all the coupled resonator structures (CRSs) can be described identically by introducing the transmission coefficient between neighboring resonators t and the free spectral range related to the period d of the CRS as

$$\omega_{\mathrm{FSR}} = \pi c/d\bar{n}. \tag{39}$$

In general the resonant frequencies and free spectral range of the resonator depend not simply on the period d but on the total phase change associated with propagating through the Bragg reflector. Similarly for ring resonators there will be a factor of π in the denominator of Eq. (39). The effective index $\bar{n}$ is chosen to adjust for this discrepancy and make (39) correct. Typically $\bar{n}$ is of the same order of magnitude as the average index of refraction and asymptotically approaches it for weak mirror reflectivity. The dispersion of CRS[6] is written as

$$\sin \pi \frac{\omega}{\omega_{\mathrm{FSR}}} = t \cos \beta d, \tag{40}$$

where t is the mirror transmission plotted in Fig. 4(d). There is a strong similarity between Fig. 4(d) and the dispersion curve for EIT (Fig. 2). In both cases the dispersion curve is "flattened" by being squeezed between two forbidden gaps. But unlike the EIT dispersion curve, the CRS dispersion curve is periodic in nature.

Introduce the order of the resonator,

$$m = \frac{\omega_0}{\omega_{\mathrm{FSR}}} = \frac{d\bar{n}}{\lambda_0/2}, \tag{41}$$

and obtain

$$\beta = \frac{2\bar{n}}{\lambda_0 m} \cos^{-1}\left(t^{-1} \sin m\pi \frac{\omega}{\omega_0}\right). \tag{42}$$

Note that the half-width of the transmission band is

$$\Omega_t = \frac{\omega_0}{m\pi} \sin^{-1} t, \tag{43}$$

and for small transmittance we can write

$$\Omega_t \approx \Omega_{t,0} = \frac{\omega_0 t}{m\pi} = \omega_{\mathrm{FSR}} \frac{t}{\pi}. \tag{44}$$

We can now find the group index as

$$n_g = c\frac{\partial \beta}{\partial \omega} = \bar{n} t^{-1} = \bar{n} \frac{\omega_0}{m\pi \Omega_{t,0}}. \tag{45}$$

Next we can find the third-order dispersion of the CRS as

$$\beta_3 = \frac{\partial^3 \beta}{\partial \omega^3} = \frac{\bar{n} m^2 \pi^2}{c\omega_0{}^2} \frac{1 - t^2}{t^3} \approx \bar{n} \frac{\omega_0}{m\pi c \Omega_{t,0}{}^3}. \tag{46}$$

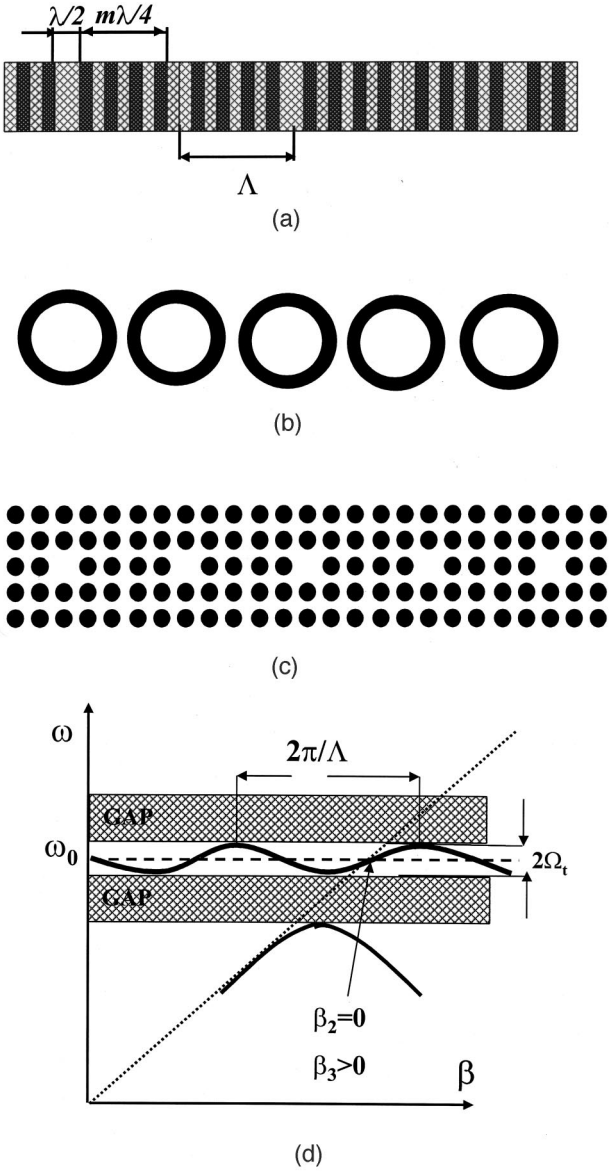

Fig. 4. Various coupled-resonator-based slow-light structures: (a) coupled Fabry–Perot cavities (Moiré pattern), (b) microring lines, (c) defect-mode waveguide in photonic crystal, (d) characteristic dispersion of CRS.

C. "Strength" of the Coupled Resonator Structure

It is important to note that the length of the period and the transmittance are related. Indeed if we assume, in the simplest case, that the period of the structure consists of one half-wavelength cavity and a reflector with $2(m-1)$ quarter-wavelength layers, the reflectivity of such a reflector is

$$r = \frac{\left(\frac{n_{\mathrm{H}}}{n_{\mathrm{L}}}\right)^{2(m-1)} - 1}{\left(\frac{n_{\mathrm{H}}}{n_{\mathrm{L}}}\right)^{2(m-1)} + 1}, \tag{47}$$

and the transmission is

$$t = (1 - r^2)^{1/2} = \frac{2\left(\frac{n_H}{n_L}\right)^{m-1}}{\left(\frac{n_H}{n_L}\right)^{2(m-1)} + 1}. \quad (48)$$

Solving Eq. (48) we obtain

$$m = 1 + \frac{\ln \frac{1 + (1 - t^2)^{1/2}}{t}}{\ln(n_H/n_L)}. \quad (49)$$

Thus for the case of small transmission (large group index) this expression can be simplified by use of Eq. (45) as

$$m \approx \frac{\ln \frac{2n_g}{\bar{n}}}{\ln \frac{n_H}{n_L}}. \quad (50)$$

Note that although expression (50) has been obtained explicitly for the Fabry–Perot-type cavities, similar dependence can be obtained for the photonic crystal (PC) resonators or microrings—in all cases the confinement length depends strongly on the index contrast available in the material system. For example, an index contrast of 1.5 and $n_g/\bar{n} \approx 100$ yields $m \approx 20$, meaning a ring radius of ≈ 5 μm at 1.5-μm wavelength, which is of the right order to avoid excessive bending losses.

Substituting Eq. (50) back into Eq. (45) we obtain the following relation between the group index and the transparency band:

$$\frac{n_g}{\bar{n}} \approx \frac{\Omega_{CRS}}{\pi \Omega_{t,0}}, \quad (51)$$

where

$$\Omega_{CRS} = \frac{\omega_0 \ln\left(\frac{n_H}{n_L}\right)}{\pi \ln \frac{2n_g}{\bar{n}}} \quad (52)$$

represents the strength of the CRS's light-slowing action in units of angular frequency, and for the third-order dispersion we obtain

$$\beta_3 \approx \frac{\Omega_{CRS}}{c\Omega_{g,0}{}^3}. \quad (53)$$

For large group indices one should take into account that the effective index itself is a function of n_g and obtain

$$\Omega_{CRS} = \frac{\omega_0 \ln\left(\frac{n_H}{n_L}\right)}{\pi \ln \frac{2n_g \ln \frac{n_g}{n_{av}}}{n_{av}}}, \quad (54)$$

where n_{av} is the average refractive index, which is only slightly different from Eq. (52).

Table 2. Performance Characteristics of Various CRS Slow-Light Optical Buffers

Structure	FBG	SiO_2–Air	Si–Air	"Ideal PC"
n_H/n_L	1.001–1.004	1.5	2.2	2.2
Ω_{CRS} (s^{-1})	3×10^{10}–3×10^{11}	1–3×10^{13}	2–6×10^{13}	2–6×10^{13}
$t^{CRS}_{scat\ max}$ (s)	10^{-6}–10^{-5}	1.5×10^{-9}	3×10^{-10}	3×10^{-9}
F_{CRS}	3×10^5	3×10^4	10^4	10^5
$N^{CRS}_{st,max}$	1600	250	160	700
$B_{max,cap}$	0.7 G[a]	180 G	450 G	220 G
Performance with storage capacity of 10 bits				
$B_{CRS,max}$	18 G	9 T	18 T	18 T
$B_{CRS,min}$	10 M	7 G	30 G	3 G
$n'_{g,max}$	10^3	200	95	775
L_{CRS} (cm)	33	0.14	0.06	0.1
Performance with storage capacity of 50 bits				
$B_{CRS,max}$	8 G	1.2 T	2 T	2 T
$B_{CRS,min}$	50 M	35 G	150 G	20 G
$n'_{g,max}$	75	25	12	75
L_{CRS} (cm)	220	1	0.5	0.7
Performance with storage capacity of 200 bits				
$B_{CRS,max}$	4 G	600 G	1 T	1 T
$B_{CRS,min}$	200 M	150 G	700 G	75 G
$n'_{g,max}$	14	6	2.5	13
L_{CRS} (cm)	1320	5	2	4

[a]Units M, G, T stand for mega-, giga-, terabits/second.

Let us now compare expressions (51) and (53) with the equivalent expressions for the EIT medium, Eq. (16) and Eq. (19), respectively. First of all, we can see that the frequency Ω_{CRS} plays the role of plasma frequency and the index contrast plays the role of oscillator strength—the higher the index contrast, the larger the group index that can be achieved. Note that although Eq. (52) is transcendental the dependence of Ω_{CRS} on the group index when $n_g \gg \bar{n}$ is much weaker than its dependence on index contrast—so for order-of-magnitude estimates Ω_{CRS} can be taken as constant.

D. Coupled Resonator Structure Performance Parameters

Let us make such a series of simple estimates. Consider first a fiber-grating type of resonator where the index contrast is of 10^{-3} or less,[29] (although there has been work with hydrogenated[30] and (or) strained[31] Ge silicate fibers in which index contrast of up to 10^{-2} has been obtained). Then for $10 < n_g/\bar{n} < 10^4$ and wavelength of 1550 nm we obtain $3\times10^{10}\ s^{-1} < \Omega_{CRS} < 3\times10^{11}\ s^{-1}$. Next let us consider a delay line made in two-dimensional SiO_2-based photonic crystal (PC)[32] where one can obtain effective index contrast of $\approx$30–40%, rendering $1\times10^{13}\ s^{-1} < \Omega_{CRS} < 3\times10^{13}\ s^{-1}$. Finally for Si[8–10,33,34] or III-V[35] semiconductor PC waveguide or microring array one can attain effective index contrast of $\approx$2.0–2.2 (considering that the low-index regions are made from either SiO_2 or from the combination of semiconductor and air holes). Thus we obtain $2\times10^{13}\ s^{-1} < \Omega_{CRS} < 6\times10^{13}\ s^{-1}$. These data are summarized in Table 2.

Thus in principle in a CRS one can attain Ω_{CRS} that is larger than Ω_p in an EIT medium. Furthermore, in the CRS the group index is inversely proportional to the passband Ω [relation (51)] while in the EIT medium the group index is inversely proportional to Ω^2 [Eq. (16)]. Therefore, it is reasonable to expect the EIT medium to outperform the CRS for narrow-bandwidth signals, while the relation is reversed for high-bandwidth signals. To quantify this we will use Eq. (20) to obtain the expression for the storage capacity:

$$N_{st} = Bt_{d,max} = \frac{\gamma^3}{B^2 c\beta_3} n_g = \frac{\gamma^3}{B^2}\frac{\omega_0^2}{m^2\pi^2}\frac{t^2}{1-t^2} = \gamma^3\frac{\Omega_{t0}^2}{B^2}\frac{n_g^2}{n_g^2-\bar{n}^2}. \tag{55}$$

Eq. (55) looks almost identical (except for a factor of 6) to the similar Eq. (22) for the EIT and leads to the similar restriction on the width of the transmission band of

$$\Omega_{t0} = \gamma^{-3/2} N_{st}^{1/2}(1-\bar{n}^2/n_g^2)^{1/2} B \approx 5.4 N_{st}^{1/2}(1-\bar{n}^2/n_g^2)^{1/2} B. \tag{56}$$

As a next step, substituting relation (56) into Eq. (45) we obtain

$$n_g = \bar{n}\frac{B_{CRS,max}}{B}(1-\bar{n}^2/n_g^2)^{-1/2} \times \frac{1}{\ln\frac{n_H}{n_L} + \ln\left[\frac{n_g}{\bar{n}}(1+\sqrt{1-\bar{n}^2/n_g^2})\right]}, \tag{57}$$

where

$$B_{CRS,max}(N_{st}) = \gamma^{3/2}\frac{\omega_0 \ln\left(\frac{n_H}{n_L}\right)}{\pi} N_{st}^{-1/2} \tag{58}$$

is the maximum bit rate at which the group velocity is slowed by a factor between 1.2 and 1.8, depending on index contrast. Now if we compare the latter two expressions with the equivalent expressions for EIT media—Eqs. (24) and (25), respectively—the similarities become clear.

Given the requirement for a delay line capable of storing N_{st} bits at bit rate B we can write

$$N_{st} = \frac{\bar{n}BL}{ct} \tag{59}$$

and substitute the bit rate from Eq. (59) into Eq. (55) to obtain

$$\frac{N_{st}^3}{\gamma^3} = \left(\frac{2\bar{n}L}{\lambda_0 m}\right)^2 (1-t^2)^{-1} = \left(\frac{L}{d}\right)^2 (1-t^2)^{-1} = N_{res}^2(1-\bar{n}^2/n_g^2)^{-1}, \tag{60}$$

where N_{res} is the total number of microresonators. Thus for a reasonably large group index we can write

$$N_{res} \approx 5 N_{st}^{3/2}, \tag{61}$$

which is a very important result. Intuitively, one might conclude that to store each bit of information at least one microresonator is required, but rigorous derivation shows that the number required is far larger because of the third-order dispersion.

We can now estimate the length of the delay line capable of storing N_{st} bits at rate B as

$$L = L_D(N_{st})\left\{\ln\frac{n_H}{n_L} + \ln\left[\frac{n_g}{\bar{n}}(1+\sqrt{1-\bar{n}^2/n_g^2})\right]\right\} \times (1-\bar{n}^2/n_g^2)^{1/2}, \tag{62}$$

where

$$L_D(N_{st}) = \frac{cN_{st}}{\bar{n}B_{CRS,max}} = \frac{\lambda_0}{2\bar{n}\ln\frac{n_H}{n_L}}\left(\frac{N_{st}}{\gamma}\right)^{3/2}. \tag{63}$$

Since L_D does not depend on the bit rate, the dependence on the bit rate is rather weak until the transmission becomes rather high. Now, note that

$$\frac{L}{L_D}\frac{B}{B_{CRS,max}} = \frac{cN_{st}/n_g}{cN_{st}/\bar{n}} = \frac{\bar{n}}{n_g}. \tag{64}$$

Substituting Eq. (64) into Eq. (62) we obtain a simple recursive relation of all the parameters:

$$\frac{L}{L_D} = \left[1-\left(\frac{L}{L_D}\frac{B}{B_{CRS,max}}\right)^2\right]^{1/2}\left\{\ln\frac{n_H}{n_L} + \ln\left[1 + \sqrt{1-\left(\frac{L}{L_D}\frac{B}{B_{CRS,max}}\right)^2}\right] - \ln\frac{L}{L_D}\frac{B}{B_{CRS,max}}\right\}. \tag{65}$$

Comparing Eq. (65) with Eq. (27) we can see a rather dramatic difference in the bit rate dependence: while the required length of an EIT buffer increases linearly with the bit rate, the length of the CRS buffer is almost bit-rate independent. The dependences on storage capacities are also different: quadratic in the EIT medium and power of 3/2 in the CRS buffer. Thus based on dispersion limitations the CRS buffer is expected to outperform greatly the EIT buffer at large bit rates and storage capacities.

Now, although as we stressed before, the main purpose of this paper is to establish the limitations on bit rates and storage capacity of optical buffers imposed by dispersion, it will still be interesting to see how these limitations combine with the limitations imposed by the loss in defining the operational region of the buffer. We have already performed these estimates for the EIT buffer [Eq. (30)]; now we can similarly define the maximum delay time for the CRS imposed by the waveguide loss per unit length α, which can be due to the combination of scattering and absorption losses,

$$t_{scat,max}^{CRS} = \ln 2(\alpha c/\bar{n})^{-1}. \tag{66}$$

Note that any decrease of group velocity is accompanied by the increase in loss, thus $t_{scat,max}^{CRS}$ stays constant.

There is one significant difference, however, between the limitations for EIT [Eq. (12)] and CRS [Eq. (66)] buffers. In the EIT medium maximum delay time is determined by the fundamental physical parameter, coherencetime, while in the CRS the maximum delay time is defined mostly by the waveguide loss, which may be significantly reduced, if not eliminated, by the progress in fabrication and processing techniques that is currently taking place. At the present time photosensitive fiber has the lowest losses, of the order of a few dB/km,[29] while the best SiO_2–air waveguides have losses of the order of 0.15 dB/cm,[36] giving maximum delay times of the order of 1500 ps, while for Si on SiO_2 the loss is of the order of 1 dB/cm, giving a maximum delay time of the order of 300 ps[37,38]; but one should expect significant improvement in the future. For this reason, we also include in Table 2 what we call here an "ideal" PC, with high index contrast and losses of 0.1 dB/cm.

By analogy with Eq. (30) we can determine the minimum bit rate for the CRS as

$$B_{\mathrm{CRS,min}}(N_{\mathrm{st}}) = N_{\mathrm{st}}/t_{\mathrm{scat,max}}{}^{\mathrm{CRS}}. \tag{67}$$

Substituting Eq. (67) into Eq. (57) we obtain the expression for the maximum value of group index attainable in the CRS delay line as

$$n_{g,\max}{}'(N_{\mathrm{st}}) = \gamma^{3/2}\frac{F_{\mathrm{CRS}}}{N_{\mathrm{st}}{}^{3/2}}, \tag{68}$$

where the finesse of the CRS line is defined as

$$F_{\mathrm{CRS}} = \Omega_{\mathrm{CRS}} t_{\mathrm{scat,max}}{}^{\mathrm{CRS}}. \tag{69}$$

We can also define the maximum storage capacity of the CRS line as the number of bits stored when the dispersion-limited maximum bandwidth [Eq. (58)] becomes equal to the loss-limited minimum bandwidth [Eq. (67)] of

$$N_{\mathrm{st,max}}{}^{\mathrm{CRS}} \approx \gamma F_{\mathrm{CRS}}{}^{2/3}. \tag{70}$$

Comparing relation (70) with Eq. (60) immediately shows that the finesse of the CRS is simply the effective number of resonators.

4. RESULTS AND DISCUSSION

We are now ready to conclude the comparison of different buffers by performing numerical solution of Eqs. (26) for five EIT buffers from Table 1 and of Eq. (65) for four CRS buffers from Table 2. Figures 5–7 correspond to storage capacities of 10, 50, and 200 bits, respectively. Each curve shows the required length of the delay line as a function of bit rate. For comparison we also show the straight line representing the required length of a simple fiber delay line, $L_{\mathrm{fib}} = c\bar{n}^{-1}N_{\mathrm{st}}B^{-1}$. Each curve has its useful frequency range between $B_{\min}$ and $B_{\max}$ emphasized by a bold section. For rates above $B_{\max}$ the velocity reduction relative to the simple fiber delay line becomes insignificant (less than twofold)—this is a fundamental limitation due to dispersion. Below $B_{\min}$ the loss becomes a major factor—this is still a fundamental limitation for the EIT medium as it is determined by the dephasing time. For the CRS delay line the loss limitation is not fundamental as it is caused only by fabrication issues—one can expect that the useful bandwidth will be expanded downward as fabrication technology progresses.

Looking at the figures one can see that the bit-rate dependences are strikingly different for EIT medium and CRS. For EIT the required length of the medium actually increases with the bit rate until the group-index enhancement becomes small, while the required length of CRS slowly decreases with bit rate. This is the expected consequence of different detuning dependences of the group indices in the two types of buffer. Clearly, at low bit rates and low storage capacities EIT media outperform the CRS buffers by a wide margin, but at higher bit rates and higher capacities the dispersion essentially eliminates the

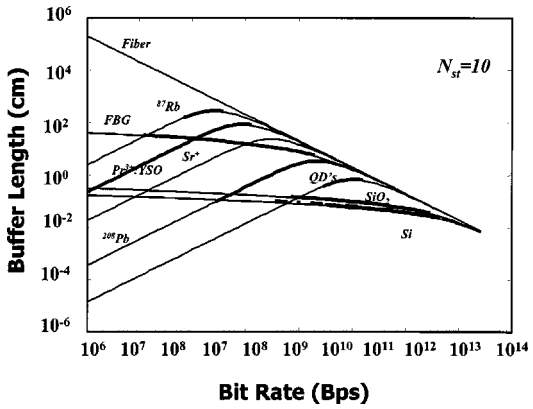

Fig. 5. Required lengths of various optical buffers with storage capacity of 10 bits as functions of bit rate. Bps bits per second.

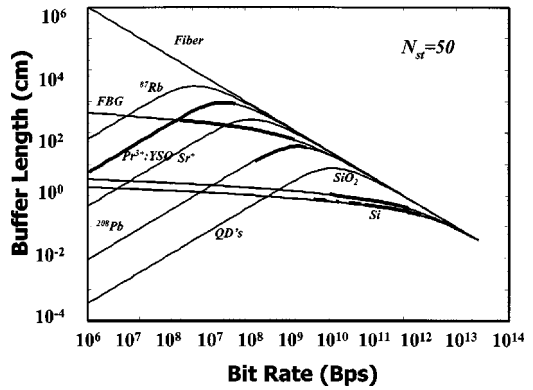

Fig. 6. Same as Fig. 5 but for 50 bits. Bps≡bits per second.

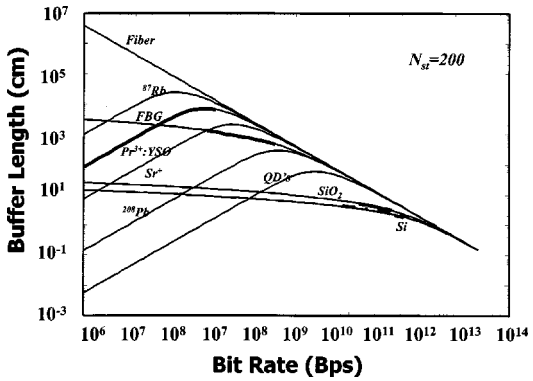

Fig. 7. Same as Fig. 5 but for 200 bits. Bps≡bits per second.

EIT capacity to slow the light, as a larger and larger transmission band is required.

For the relatively low storage capacity of 10 bits (Fig. 5) one can see that of three metal-vapor EIT media only the Pb vapor appears to be practical, i.e., capable of storing 10 bits in a length less than 1 cm for bit rates in the 0.2–20 gigabits/s range. Although originally suggested by Harris *et al.*[15] the EIT in this medium was achieved at much weaker atomic density, and only one bit was stored.[16] At the same time, of the other media in which EIT has been demonstrated, Rb and Sr vapors seem to be unable to store even 10 bits of information in a short length without incurring undue loss. The solid medium PrYSO, because of its low loss, is capable of storing 10 bits but only at low bit rates. Once the bit rate exceeds 10 megabits/s the required buffer length exceeds a few centimeters, i.e., becomes impractical (unless one can embed Pr ions into the fiber while keeping long dephasing times). The proposed QD EIT medium shows promise in the range around 10 gigabits/s but only under the assumption of long (hundreds of picoseconds) coherence times. With more realistic coherence times of the order of less than a picosecond the QD medium also becomes impractical.

For the CRS buffer the situation is different; the low-index-contrast-fiber-Bragg-grating (FBG)-coupled resonator line offers good performance for bit rates of up to 20 gigabits/s in a few tens of centimeters' length. Although currently the FBG length rarely exceeds a few centimeters, hopefully one day a meter-long grating may become feasible. The coupled resonators made in SiO_2 and Si offer good performance in the 10 gigabits/s–10 terabits/s range with group-velocity reduction by up to two orders of magnitude.

As one moves to a more useful storage capacity of 50 bits (Fig. 6) one can see that only PrYSO maintains some degree of practicality, as it appears to be able to slow light by a significant factor at low bit rates of up to 1 megabit/s all in a length of a few centimeters. For the Pb vapor the minimum required length is more than 10 cm, which renders it impractical. The QDs, because of a combination of loss and dispersion, appear not to be able to store all that many bits (in accordance with Table 1).

Among the CRS buffers the FBG line is still able to function in a wide range of bit rates, from 0.1 to 10 gigabits/s with a slowing factor of nearly 200 at the low end of this range. The silica structures have a useful bandwidth range between 200 gigabits/s and 1 terabit/s and a maximum group-index enhancement of $\approx$20. The highest index-contrast-semiconductor structures have their range limited to a few tens of terabits/s and maximum index enhancement of the order of 10. At the same time, if the loss in Si CRSs can be reduced to less than 0.1 dB/cm ("ideal structure") the useful bit-rate region (shown in a section of dashed line) expands to cover two octaves (from 20 to 2,000 gigabits/s), and the maximum group-index enhancement at 20 gigabits/s approaches 75.

Finally, expanding the storage capacity to 200 bits (Fig. 7) renders all the EIT buffers ineffective beyond 1 megabit/s; the only medium unimpeded by absorption, PrYSO, would need to be meters long. The FBG structure also loses its effectiveness since only a fewfold reduction in group velocity can now be attained, and the required length of the grating approaches a few meters. Of all the high-index-contrast structures only the "ideal PC" made of high-index semiconductor with air bridge and low (0.1 dB/cm) losses potentially offers sufficient (tenfold) group-velocity reduction in the range of a few hundred gigabits/s.

5. CONCLUSIONS

In this work we have performed rigorous comparative analyses of two types of slow-light media that are currently being considered for use in optical delay lines: EIT media and CRSs. We have pointed out the similarities and differences between these two approaches. These similarities and differences are conveniently summarized in Table 3. Let us reiterate them.

In both EIT and CRS media the slowing action takes place as a result of strong resonant interaction between either electromagnetic field and polarizable medium (EIT) or between two or more electromagnetic waves (CRS). The strength of interaction determines both the degree to which the group velocity can be reduced (group index) and the maximum bit rate at which the group-velocity reduction can be achieved. In the case of EIT the interaction strength is determined by plasma frequency, i.e., the combination of density of active atoms and their oscillator strength, while in CRSs the strength is determined primarily by the index contrast. The EIT interaction strength in units of angular frequency spans the range of 10^{10} s^{-1} in rare-earth-doped materials to 10^{12} s^{-1} in prospective QD buffers. The CRS interaction strength ranges from 10^{10} s^{-1} in resonators comprised of FBGs to 5×10^{13} s^{-1} in high-index-semiconductor structures. The stronger interaction in CRSs relative to EIT indicates that higher bit rates are attainable in them.

In both EIT and CRSs one can introduce a figure of merit, finesse, that determines their maximum storage capacity. Finesse can be loosely interpreted as a number of interactions that occur within a characteristic decay time. In the case of EIT that time is the decoherence time of the forbidden transition $G\rightarrow B$, while in CRSs it is the scattering–absorption time. Typically the "weaker" optical delay media, such as PrYSO or FBG-based resonators, have higher finesses and storage capacities, but they can be realized at lower bit rates. It is hoped that progress in fabrication of high-index photonic structures will extend the storage capacity of CRSs.

The main difference between EIT media and CRSs lies in the relations between the group index n_g, third-order dispersion β_3, and transparency bandwidth 2Ω. The stronger (Ω^{-2} versus Ω^{-1}) dependence of the EIT group index shows that spectacular index reduction can be achieved at low bit rates in the EIT medium, as supported by numerous experiments.[16–18] But EIT media also have stronger third-order-dispersion dependence on transmission bandwidth. As a result their ability to slow light falls drastically with an increase in bit rate. In fact the required length of the EIT delay line increases with an increase in bit rate, while the length of CRS delay line decreases. Herein lie inherent advantages of CRS optical buffers.

Table 3. Comparison of EIT and CRS Slow-Light Optical Buffers

Parameter	EIT	CRS
Strength of resonant interaction	$\Omega_p = \left(\frac{Ne^2 f_{AG}}{4\bar{n}^2 m_0 \varepsilon_0}\right)^{1/2}$; $10^{10}-10^{12}$ s^{-1}	$\Omega_{CRS} = \frac{\omega_0 \ln\left(\frac{n_H}{n_L}\right)}{\pi \ln\frac{2n_g}{\bar{n}}}$; $10^{10}-5\times10^{13}$ s^{-1}
Finesse	$F_{EIT} = 1/2\Omega_p T_2$; 10^2-10^7	$F_{CRS} = \Omega_{CRS}\bar{n}c^{-1}\alpha^{-1}$; $10^4-3\times10^5$
Maximum storage capacity	$N_{st,max} = \frac{\gamma}{6^{1/3}}F^{2/3}$; $1-10^4$	$N_{st,max}^{CRS} \approx \gamma F_{CRS}^{2/3}$; 160–1600
Transparency bandwidth	2Ω	$2\Omega_{t,0} = 2\frac{\omega_0 t}{m\pi}$
Group index	$\frac{n_g^{(EIT)}}{\bar{n}} = 1 + \frac{\Omega_p^2}{\Omega^2}$	$\frac{n_g}{\bar{n}} \approx \Omega_{CRS}/\pi\Omega_{t,0}$
Third-order dispersion	$\beta_3^{(EIT)} = \frac{6\Omega_p^2 \bar{n} c^{-1}}{\Omega^4}$	$\beta_3^{(CRS)} \approx \frac{\Omega_{CRS}}{c\Omega_{t,0}^3}$
Maximum effective bit rate for given storage capacity	$B_{EIT,max}(N_{st}) = \frac{\gamma^{3/2}}{6^{1/2}}\Omega_p N_{st}^{-1/2}$	$B_{CRS,max}(N_{st}) \approx \gamma^{3/2}\Omega_{CRS}N_{st}^{-1/2}$
Minimum length of buffer for given storage capacity and bit rate	$L_{EIT}(N_{st},B) \approx \frac{6c}{\gamma^3\bar{n}}\frac{N_{st}^2 B}{\Omega_p^2}$	$L_D(N_{st}) = \frac{cN_{st}}{\bar{n}B_{CRS,max}} = \frac{c}{\bar{n}\Omega_{CRS}}\left(\frac{N_{st}}{\gamma}\right)^{3/2}$

Let us now take a final look at the results developed in this work and try to answer two simple questions: Is there a place for slow-light optical buffers in optical communication–processing, and what type of medium best fits the requirements?

For the EIT-type buffers notwithstanding their main advantage (ability to vary delay continuously), the answer is unequivocally negative. One may achieve spectacular slowing at kilobit/second rates, but for bit rates in excess of 1 megabit/s and storage capacities of more than a dozen bits, all EIT buffers appear to be ineffective because of their high dispersion. Even if the coherence time is increased, by use for instance of spin coherence,[39] the dispersion still will not allow high-bit-rate applications. This forlorn conclusion is based entirely on dispersion considerations, before all the practical difficulties (requirements for strong pump laser and inconvenient wavelength) are taken into account. That, of course, does not negate the fact that EIT-induced slow light has many scientific applications where delaying–stopping a single bit of information at any bit rate may prove valuable, such as for example in quantum optics.

For the CRS optical buffer the answer is more qualified. It seems that there exist two niches open for CRS at different ranges of bit rates. One such niche is FBG-based coupled resonators in the 1–10-gigabit/s range. One can envision that by using high-index (up to 0.5%) gratings that are up to a meter long one can store up to 100 bits of information in it—a task that would require an unstructured fiber of 50 m. The second niche is in future high-speed systems operating at hundreds of gigabits/s. For this niche structures with high index contrast and low losses need to be developed from Si and other semiconductors with air bridge technology. Then small delay elements can be formed capable of storing hundreds of bits of information in a less-than-1-cm path length. Note that at present, fabrication technology is about two orders of magnitude away from achieving such losses, but rapid progress is being made. An alternative to loss reduction could be using a semiconductor medium with optical gain that could be traditional or Raman-pumped. But even with these future structures the group index cannot be expected to exceed a factor of more than 10–50 or so unless some means to mitigate the dispersion is employed. Such means may include combining coupled resonator lines having positive β_3 with all-pass filters having negative β_3, as recently proposed,[40] or other still unexplored methods, such as making CRSs from EIT media. In addition, to attain practicality, the need to control the delay by use of nonlinear optical or electro-optical means should be addressed. Recent results[41] are encouraging.

In conclusion, we have investigated how third-order dispersion severely limits the performance of various types of slow-light optical buffers at high bit rates and

shown that high-index-contrast CRSs hold an advantage over EIT-type media.

REFERENCES

1. R. Langenhorst, M. Eiselt, W. Pieper, G. Grosskopf, R. Ludwig, L. Kuller, E. Dietrich, and H. G. Weber, "Fiber loop optical buffer," J. Lightwave Technol. **14**, 324–335 (1996).
2. G. Lenz, B. J. Eggleton, C. K. Madsen, and R. E. Slusher, "Optical delay lines based on optical filters," IEEE J. Quantum Electron. **37**, 525–532 (2001).
3. M. Scalora, R. J. Flynn, S. B. Reinhard, and R. L. Fork, "Ultrashort pulse propagation at the photonic band edge: Large tunable group delay with minimal distortion and loss," Phys. Rev. E **54**, R1078–R1081 (1995).
4. C. K. Madsen and G. Lenz, "Optical all-pass filters for phase response design with applications for dispersion compensation," IEEE Photonics Technol. Lett. **10**, 994–996 (1998).
5. M. Soljacic, S. G. Johnson, S. Fan, M. Inanescu, E. Ippen, and J. D. Joannopulos, "Photonic-crystal slow-light enhancement of nonlinear phase sensitivity," J. Opt. Soc. Am. B **19**, 2052–2059 (2002).
6. A. Melloni, F. Morichetti, and M. Martnelli, "Linear and nonlinear pulse propagation in coupled resonator slow-wave optical structures," Opt. Quantum Electron. **35**, 365–378 (2003).
7. Z. Wang and S. Fan, "Compact all-pass filters in photonic crystals as the building block for high-capacity optical delay lines," Phys. Rev. E **68**, 066616–066623 (2003).
8. Y. Tao, Y. Sugimoto, S. Lan, N. Ikeda, Y. Tanaka, and Y. K. Asakawa, "Transmission properties of coupled-cavity waveguides based on two-dimensional photonic crystals with a triangular lattice of air holes," J. Opt. Soc. Am. B **20**, 1992–1998 (2003).
9. S. Nishikawa, S. Lan, N. Ikeda, Y. Sugimoto, H. Ishikawa, and K. Asakawa, "Optical characterization of photonic crystal delay lines based on one-dimensional coupled defects," Opt. Lett. **27**, 2079–2081 (2002).
10. Y. Sugimoto, S. Lan, S. Nishikawa, N. Ikeda, H. Ishikawa, and K. Asakawa, "Design and fabrication of impurity band-based photonic crystal waveguides for optical delay lines," Appl. Phys. Lett. **81**, 1948–1950 (2002).
11. N. M. Litchinitser, B. J. Eggleton, and G. P. Agrawal, "Dispersion of cascaded fiber gratings in WDM lightwave systems," J. Lightwave Technol. **16**, 1523–1529 (1999).
12. J. B. Khurgin, "Light slowing down in Moire fiber gratings and its implications for nonlinear optics," Phys. Rev. A **62**, 3821–3824 (2000).
13. A. Yariv, Y. Xu, R. K. Lee, and A. Scherer, "Coupled-resonator optical waveguide: a proposal and analysis," Opt. Lett. **24**, 711–713 (1999).
14. K.-J. Boller, A. Imamoglu, and S. E. Harris, "Observation of EIT," Phys. Rev. Lett. **66**, 2593–2596 (1991).
15. S. E. Harris, J. E. Field, and A. Kasapi, "Dispersive properties of EIT," Phys. Rev. A **46**, R29–R32 (1992).
16. A. Kasapi, M. Jain, G. Y. Jin, and S. E. Harris, "EIT: Propagation dynamics," Phys. Rev. Lett. **74**, 2447–2450 (1995).
17. L. V. Hau, S. E. Harris, Z. Dutton, and C. H. Behroozi, "Light speed reduction to 17 metres per second in an ultracold atomic gas," Nature **397**, 594–596 (1999).
18. M. M. Kash, V. A. Sautenkov, A. S. Zibrov, L. Hollberg, G. R. Welch, M. D. Lukin, Y. Rostovtsev, E. S. Fry, and M. O. Scully, "Ultraslow group velocity and enhanced nonlinear optical effects in a coherently driven hot atomic gas," Phys. Rev. Lett. **82**, 5229–5232 (1999).
19. A. V. Turukhin, V. S. Sudarshanam, and P. R. Hemmer, "Observation of ultraslow and stored light in a solid," Phys. Rev. Lett. **88**, 023602–1-4 (2002).
20. M. Bajcsy, A. S. Zibrov, and M. D. Lukin, "Stationary pulses of light in an atomic medium," Nature (London) **426**, 638–641 (2003).
21. D. F. Phillips, A. Fleischhauer, A. Mair, R. L. Walsworth, and M. D. Lukin, "Storage of light in atomic vapor," Phys. Rev. Lett. **86**, 783–786 (2001).
22. P. C. Ku, C. J. Chang-Hasnain, and S. L. Chuang, "Variable semiconductor all-optical buffers," Electron. Lett. **38**, 1581–1583 (2002).
23. N. W. Ashcroft and N. D. Mermin, *Solid State Physics* (Saunders, New York, 1996), p. 551.
24. Y.-Q. Li and M. Xiao, "EIT in 3-level Λ-type system in Rb atoms," Phys. Rev. A **51**, R2703–R2706 (1995).
25. M. S. Bigelow, N. N. Lepeshkin, and R. W. Boyd, "Observation of ultraslow light propagation in a ruby crystal at room temperature," Phys. Rev. Lett. **90**, 113903–113904 (2003).
26. M. D. Lukin, M. Fleichhauer, A. S. Zibrov, and M. O. Scully, "Spectroscopy in dense coherent media: line narrowing and interference effects," Phys. Rev. Lett. **79**, 2959–2962 (1997).
27. R. W. Equal, R. L. Cone, and R. M. MacFarlane, "Homogeneous broadening and hyperfine structure of optical transitions in $Pr^{3+}:Y_2SiO_5$," Phys. Rev. B **52**, 3963–3970 (1995).
28. G. P. Agrawal, *Fiber Optic Communication Systems*, 3rd ed. (Wiley, New York, 2002), p. 51.
29. A. Othonos and K. Kalli, *Fiber Bragg Gratings* (Artech House, Norwood, Mass., 1999), p. 220.
30. P. J. Lemaire, "High pressure H_2 loading as a technique for achieving ultrahigh UV photosensitivity and thermal sensitivity in GeO_2 doped optical fibers," Electron. Lett. **29**, 1191–1193 (1991).
31. E. Salik, D. S. Starodubov, V. Grubsky, and J. Feinberg, "Increase of photosensitivity in Ge-doped fibers under strain," in *Optical Fiber Communications Conference*, Postconference Digest, Vol. 37 of OSA Trends in Optics and Photonics Series (Optical Society of America, Washington, D.C., 2000), pp. 124–125.
32. M. R. Poulsen and P. I. Borel, "Advances in silica based integrated optics," Opt. Eng. (Bellingham) **42**, 2821–2856 (2003).
33. M. Notomi, K. Yamada, A. Shinya, J. Takajhashi, and I. Yokohama, "Extremely large group-velocity dispersion of line-defect waveguides in photonic crystal slabs," Phys. Rev. Lett. **87**, 235902–1-4 (2001).
34. Yu. A. Vlasov and S. J. McNab, "SOI 2D photonic crystals for microphotonic integrated circuits," in *2003 Digest of the LEOS Summer Topics Meetings* (Institute of Electrical and Electronics Engineers Lasers and Electro-Optics Society, Piscataway, N.J., 2003), p. 79.
35. N. Carlsson, N. Ikeda, Y. Sugimoto, K. Asakawa, T. Takemori, Y. Katayama, N. Kawai, and K. Inoue, "Design, nano-fabrication and analysis of near-infrared 2D photonic crystal air-bridge structures," Opt. Quantum Electron. **34**, 123–130 (2002).
36. L. Tong, R. Gattass, J. Ashcom, S. He, J. Lou, M. Shen, I. Maxwell, and E. Mazur, "Subwavelength-diameter silica wires for low-loss optical wave guiding," Nature (London) **426**, 816–819 (2003).
37. S. J. McNab, N. Moll, and Yu. A. Vlasov, "Ultra-low loss photonic integrated circuit with membrane-type photonic crystal waveguides," Opt. Express **11**, 2927–2939 (2003), http://www.opticsexpress.org.
38. Yu. A. Vlasov and S. J. McNab, "Losses in single-mode silicon-on-insulator strip waveguides and bends," Opt. Express **11**, 2927–2939 (2003), http://www.opticsexpress.org.
39. T. Li, H. Wang, N. H. Kwong, and R. Binder, "EIT via electron spin coherence in QW waveguide," Opt. Express **11**, 3298–3303 (2003), http://www.opticsexpress.org.
40. J. B. Khurgin, "Expanding the bandwidth of slow light photonic devices," Opt. Lett. **30**, 513–515 (2005).
41. M. F. Yanik and S. Fan, "Stopping light all-optically," Phys. Rev. Lett. **92**, 083901–083904 (2004).